**Journal of Fusion Energy manuscript No.**
(will be inserted by the editor)

# Physical and numerical model for calculation of ensembles of trajectories of dust particles in a tokamak

**Gabriele Gervasini · Enzo Lazzaro · Andrea Uccello**

Received: date / Accepted: date

**Abstract** The calculation of the trajectories and main physical parameters (e.g. mass, temperature, electric potential) of an ensemble of several representative dust particles has recently emerged as an important problem in the physics of tokamaks, with the aim of studying their role as a source of impurities in a thermonuclear plasma and their effects in the interaction with the first wall. The physical problem despite its apparent simple goals, is fraught with difficulties related to various subtle physical processes and requires the development of specific accurate numerical tools. In this work, the key physics aspects of the problem of dust tracking in a high temperature tokamak plasma are addressed from the concrete point of view of developing adequate and consistent numerical tools for their treatment. The basic elements and the rationale of the numerical code DUST-TRACKing (DUSTTRACK) developed for it are outlined. To describe the performance and potential of DUSTTRACK, a "realistic" output of the code is finally showed.

**Keywords** DUSTTRACK · nuclear-fusion · tokamak · dust

G. Gervasini
Istituto di Fisica del Plasma IFP-CNR, Via Roberto Cozzi 53, 20125, Milan, Italy

E. Lazzaro
Istituto di Fisica del Plasma IFP-CNR, Via Roberto Cozzi 53, 20125, Milan, Italy

A. Uccello
Istituto di Fisica del Plasma IFP-CNR, Via Roberto Cozzi 53, 20125, Milan, Italy
Tel.: +39-02-66173231
Fax: +39-02-66173237
E-mail: uccello@ifp.cnr.it

## 1 Introduction

Burning plasmas of nuclear fusion tokamak devices will generate intense thermal loads (up to 10 $MW/m^2$) and high particles fluxes (up to $10^{24}$ $m^{-2}s^{-1}$ for hydrogen isotopes) which ultimately interact with a material boundary of the so-called Plasma Facing Components (PFCs) [1]. This harsh environment unavoidably leads to PFCs sputtering and eventually to the production of mobilizable solid particulate or dust [2,3,4]. Dust particles, moving almost freely in the tokamak vessel, constitute a source of impurity of the plasma leading to an increase of radiation power losses and plasma dilution [5,6,7]. The issue of dust in tokamaks also has important implications in terms of nuclear fusion reactor safety due to it's chemical activity, toxicity, tritium retention, and radioactive content [8].

Characterization studies following experimental campaigns enabled to define some ranges of parameters for dust particles in tokamaks [2,9]. Specifically, they have a large variety of shapes (from irregular elongated to spherical) and sizes (from few nm to few hundred $\mu$m). Moreover, their composition obviously reflects that of the particular configuration of PFCs and plasma of the device considered.

In order to improve the understanding of dust-related phenomena in tokamaks, the setting up of dedicated and validated numerical modeling tools is required. Among these, a useful role is played by the dust trajectory calculators, which can present in a relatively clear way qualitative and quantitative description of the mobilization and fate of selected bunches of dust grains [10, 11,12,13,14,4,15,16,17]. The purpose of this class of codes is to perform off-line analysis of dynamics of dust samples in real tokamak shots, interfacing with the available data, i.e. equilibrium configuration and plasma profiles, static or time dependent, in a region bounded by the first wall and PFCs and the plasma boundary defined either by a magnetic separatrix or by contact conditions with a limiter. In the following we shall discuss the basic ordering of the effects which have implications on the physics problems and the efficiency of numerical techniques.

Although there are several papers in literature which describe the different dust trajectory calculators (e.g. [12,13] for DTOKS, [10,11] for DUSTT and [4, 15,16] for MIGRAINe), they focus almost exclusively on the physics models of such codes lacking of some important technical details about the numerics and computational strategies adopted which could be very helpful to the other developers.

In this work, contextually with the discussion of how to approach the dust transport issues from a physical point of view, we present the key aspects of the architecture of the code DUST-TRACKing (DUSTTRACK) [17] developed to address computationally the dynamics of test dust particles in realistic tokamak devices. The code is written in Fortran 90 language and runs on Unix-like systems. The physics modules of DUSTTRACK are built from separately tested parts and new ones can be easily added. These modules can be continually updated and extended as improved physics models or more ef-

ficient algorithms are developed. The emphasis in this project is to implement appropriate compromises between efficiency and accuracy, and to assess the physical approximations made, in order to ease any check of correctness and provide modules that can usefully be employed in a tokamak dust transport code.

Starting with a brief overview of the general topic of dust transport in tokamaks (section 2), the main features of the code DUSTTRACK and of its physics model are presented (section 3). The paper then moves on to the description of the DUSTTRACK input information (section 4) and its architecture with the approach used to address several numerical problems (section 5). The main results of the code are presented (section 6) as paradigmatic examples typical of contemporary tokamaks such as the Joint European Torus (JET, Culham, Oxfordshire, United Kingdom) and the Axially Symmetric Divertor EXperiment (ASDEX Upgrade, Garching, Germany). Finally, some conclusions are drawn (section 7).

## 2 Fusion plasma

The typical framework for the investigation of dust dynamics in tokamaks is shown in figure 1a, which depicts the poloidal cross-section of JET in its divertor configuration. The image highlights the presence of two plasma re-

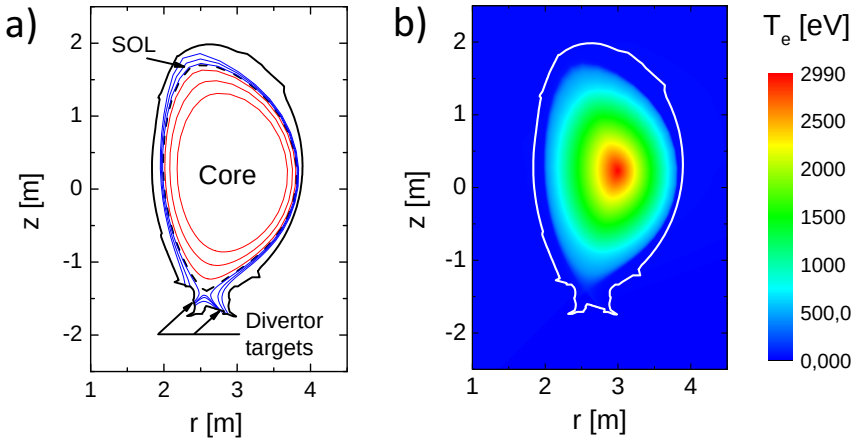


**Fig. 1** (a) Cross-section and magnetic geometry of JET. The chamber (solid black line), a set of closed and open magnetic field lines (red and blue solid lines) and the Last Closed Magnetic Surface LCMS (black dashed line), as extracted from the "EQDSK" file [18], are shown. (b) Example of JET plasma electron temperature $T_e$ (in electronvolt, eV) profile as computed with EDGE2D [19, 20] and extrapolated till the core and the chamber (see section 4). JET plasma pulse (or "shot") #82806 at 55-56 s is here considered.

gions: the central hot region ($\sim 10^8$ K), or "core", and the boundary region, or

"Scrape-Off-Layer" (SOL). Nuclear fusion takes place in the dense core, where the magnetic surfaces are closed isobars and the charged plasma species are well confined. The SOL, on the contrary, is a layer of plasma, of width dictated by diffusion-convection processes, tied to open field lines which are connected ("diverted") to the solid structure of contact with the plasma: the divertor. The "separatrix" (not shown in figure 1a for readability) is the magnetic surface, characterized by a singular point where the poloidal field vanishes and separates the closed confinement isobaric surfaces from the bundle of SOL field lines which intersects the tokamak vessel, namely on the "divertor plates". Due to several mechanisms, the core plasma unavoidably diffuses out to the SOL [21]. Most plasma losses (in terms of particles and heat fluxes) occur along the magnetic field lines to the divertor targets. The remaining non-diverted plasma diffuses perpendicularly to the magnetic surfaces and eventually impinges on the vessel wall. Plasma hitting surfaces causes their erosion with consequently injection of divertor and wall materials into the plasma itself.

In addition to influx of atomic or ionic impurity species, some of the debris material may consist of "dust" particles of size ranging from nanometers to micrometers, which can penetrate in the SOL as well as being deposited on the PFCs as thin films [22]. The flaking of these films may be another source of dust particles in the plasma. The nature of these phenomena necessarily leads to dust particles mainly containing materials used for divertor targets, chamber wall and other structural elements, which are typically graphite, tungsten (W), beryllium (Be) and constituents of steel and Inconel (i.e. iron, nickel, chromium).

Clearly, the origin and behavior of dust particles in tokamaks are intimately connected to the specific magnetic geometry and ambient plasma parameters (i.e. temperature, density and velocity) which can influence dust charging, acceleration and ablation. Realistic studies of dust dynamics require full information of the details of the axisymmetric equilibrium magnetic flux surfaces and SOL, for specific experimental cases. These are typically available in "EQDSK" format [18], including essential geometric details of the vacuum vessel and PFCs (figure 1a). The data contained into the EQDSK constitute also the input of the SOL transport codes, e.g. EDGE2D [19,20], through which the spatial steady-state distributions of plasma and impurities parameters can be obtained (figure 1b).

## 3 DUSTTRACK physics model

The main objective of DUSTTRACK is the calculation of the trajectories of a collection of several representative, isolated spherical dust particles, to gain information on their distribution in the SOL as well as their role as source of impurities, when eventually reaching the interior, hotter region of the SOL. As it will become clear later, the trajectories of the dust particles in a tokamak do not depend only on the ambient electromagnetic fields and plasma properties but are also determined by the evolution of the dust particles main physical

parameters, i.e. temperature $T_d$, surface electric potential $\phi_d$ (or, equivalently, the surface charge $q_d$) and mass $M_d$. The neglect of the dust-dust interactions is justified for micrometer-sized particles with a low number density $n_d$, so that the interparticle distance $\Delta \propto {n_d}^{-1/3} >> \lambda_d$, the Debye length. In these conditions an appropriate mathematical model consists of a set of several coupled time Ordinary Differential Equations (ODEs) for each particle. The dynamics of a finite size dust particle should be studied in terms of the motion of its Center of Mass (C.M.) and the intrinsic rotation around an axis through it. Now, for the purposes of dust interaction with tokamak SOL and PFCs, the role of the intrinsic mechanical degrees of freedom is marginal. For instance, in this context the particle spinning around an axis through its C.M. has no leading order effect in the (dominant) drag force, nor in the particle charging processes though the Coulomb cross sections. Therefore, for the effects to be analyzed, the C.M. motion is the most important and in DUSTTRACK the Newton's equations for the C.M. variables (position $\mathbf{x}_d$ and velocity $\mathbf{v}_d$) are solved together with an ODE for each of the dust physical parameters. One of the distinguishing properties of DUSTTRACK is its capability of following simultaneously the dynamic evolution of an ensemble (even large) of particles and not one at a time as the other trajectory calculators (see section 5). This feature allows to construct much more efficiently statistical analyses both in a data interpretation or in a predictive mode. Clearly the "ensemble" approach is also less time consuming and can be extended also to consider weak particles interactions.

Additional time-dependent variables, other than $\mathbf{x}_d$, $\mathbf{v}_d$, $T_d$, $\phi_d$ and $M_d$ (the "basic" ones), can be also included by providing the relevant differential equations for their time behavior. In this work, only the basic time-dependent quantities are considered. Among these, the equations for intrinsic rotation could be activated, if necessary. Actually, spinning could result from inelastic collisions with the wall, viscous torque in the plasma, quickly damped, and a magnetic torque $\mathbf{m}_d \times \mathbf{B}$ due to an acquired magnetic dipole moment $\mathbf{m}_d$. Indeed a spherical particle with a net charge, spinning with frequency $\omega$, has a magnetic dipole moment $m_d = q_d \omega R_d^2$ (where $R_d$ is the dust particle radius), which could be subject to an additional $\nabla\mathbf{B}$ force ($\mathbf{F}_{\nabla\mathbf{B}}$), similar to that of ferromagnetic dust. However the order of magnitude of the ratio of this force over the gravitational force is expected to be about $10^{-13}$ therefore totally negligible. Nonetheless since the $\mathbf{F}_{\nabla\mathbf{B}}$ for ferromagnetic particles is already included in the code, it is a viable option to turn-on, when necessary, a (charge dependent) "equivalent" magnetic moment proportional to the spinning frequency (i.e. very small).

All of this leads to three major physics modules which constitute DUSTTRACK: the charging module (subsection 3.1), the heating module (subsection 3.2) and the active force module (subsection 3.3). The non-trivial nature of the problem of dust particles dynamics in tokamaks is made further complex by considering the unavoidable collisions between dust grains and PFCs, i.e. the boundary of DUSTTRACK physical domain. A fourth module was

therefore implemented to take into account the reflections of dust particles from tokamak chamber (subsection 3.4).

Although as a first approximation, the vessel of tokamaks can be considered axisymmetric, in reality, its geometry is quite complicated because of the presence of various components, such as discrete protection tiles and baffles, with recessed and protruding elements, as well as plasma diagnostics and control equipment. These three-dimensional (3D) features can strongly affect the trajectories of the dust particles (in terms of the dust-wall reflections geometry). They could also constitute important accumulation regions from which the dust particles can be mobilized. For greater simplicity of modeling (and a safer numerical implementation) in complicated geometry (even non-axisymmetric like those of stellarators), the calculations in DUSTTRACK are carried out in a 3D Cartesian coordinate system. This approach is a simple but useful choice considering that all the other main codes [10,11,12,13,4,15, 16] employ cylindrical and toroidal coordinate systems, very suitable for the axisymmetric approximation of tokamaks.

The DUSTTRACK physics model has been developed considering that the input temperature and density profiles of the various background plasma species present (electrons, ions and neutrals) as well as the flow profiles are read in from the experimental files, preprocessed by SOL transport codes, such as EDGE2D [19,20], and eventually extrapolated to the core and the vessel, or alternatively, for testing purposes, from analytical models programmed as suitable functions (see section 4).

### 3.1 The charging module

The discussion starts considering the dust charging physics model. It aims to evaluate the dust particles' floating potential $\phi_d$ which determines the fluxes of charged plasma species and impurities reaching the dust particles surface, thus playing a key-role in the calculation of the forces experienced by the dust particles and ultimately their trajectories. Thanks to the achieved numerical robustness of DUSTTRACK, the dust charging process is described by a (non-linear) ODE, differently from others [11,12,13,15], who use the steady state (ambipolarity) condition. This procedure is numerically more accurate and efficient in comparison with an iterative root-finding method for the steady state condition. The elementary dust grain charging time is extremely fast, of the order of the inverse ion plasma frequency, but a possibly evolving background affects the time variation of the charging process. Actually, the charging ODE is written for the dust charge $q_d$, estimated from $\phi_d$ following the well-known formula for spherical capacitors $\phi_d = q_d/(4\pi\epsilon_0 R_d)$. The current associated to the absorption of the charged plasma species, $I_{plasma}$, is evaluated following the commonly used Orbital Motion Limited (OML) approach for spherical dust particles [23,24]. Moreover, in fusion plasmas, the high energy of charged plasma species and the significant power reaching the dust grains impose to consider also Secondary Electron Emission (*SEE*, $I_{SEE}$) and ThermIonic emis-

sion ($TI$, $I_{TI}$) as further charging mechanisms. $I_{TI}$ is expressed through the Richardson-Dushman formula [25] properly corrected to take into account the Schottky effect for $q_d < 0$ and the fraction of the emitted electrons pulled back to the dust grain, which do not contribute to the compute of $I_{TI}$, when $q_d > 0$ [26]. The SEE mechanism is well described by the $\delta_{SEE}$ yield, which corresponds to the number of secondary electrons the dust grain emits when it is hit by an electron (no other impinging species is considered). It is a function of the electron energy and incidence angle and is assumed separable with respect to these two variables. For the dependance on energy at normal incidence the Kollath's semi-empirical formula is used [27]. The angular part is modeled following [28]. In order to find $I_{SEE}$, $\delta_{SEE}$ is numerically integrated over the assumed Maxwellian energy distribution of incoming electrons. As for the TI emission, when $q_d > 0$, some secondary electrons are eventually trapped and recollected by the dust. Such electrons do not contribute to $I_{SEE}$ and a corrective factor is included [29].

### 3.2 The heating module

The heating module calculates the thermal power received by the dust grain ($Q_{tot}$), which plays a major role in the variation of the dust particle temperature $T_d$, thus governing possible phase transitions (i.e. sublimation, melting, boiling and surface evaporation), responsible for the specific distribution of the source of impurities in the plasma. Considering the heating process as isobaric, DUSTTRACK equates $Q_{tot}$ with the rate of change of dust particle enthalpy ($dH_d/dt$). The ODE for $T_d$ is written substituting $H_d$ with the relation $M_d c_{p,d} T_d$ (where $c_{p,d}$ is the specific heat at constant pressure of the dust material). $Q_{tot}$ is the sum of different contributions: the power received by the dust grain through plasma species absorption ($Q_{plasma}$), the power emitted by the dust grain via SEE, TI and black-body emissions ($Q_{SEE}$, $Q_{TI}$ and $Q_{rad}$, respectively) and the loss of power due to dust gas phase transitions ($Q_{gas}$). $Q_{plasma}$ ($Q_{SEE}$ and $Q_{TI}$) is (are) calculated averaging the flux of energy of the absorbed (emitted) particles over their energy distributions. As for $I_{plasma}$, $Q_{plasma}$ is evaluated using the OML approach. $Q_{SEE}$ assumes the energy distribution of [29] for the SEE electrons and the TI electrons are modeled through a Maxwellian distribution with the dust temperature $T_d$. The thermal radiation power of the dust particle $Q_{rad}$ is described by the Stefan-Boltzmann law.

Given the high temperatures in the inner SOL, dust grains undergo bulk phase transitions (i.e. sublimation, melting and boiling) rather quickly approaching that region. Moreover, due to the small pressure inside the tokamak chamber (e.g. $1 \div 10$ Pa in the divertor region of the under-construction ITER [30]), also dust surface evaporation has to be taken into account, whose impact on the dust mass decrease becomes strong from temperatures of the order of some thousand of K for typical plasma facing materials. The DUSTTRACK heating module is therefore completed with a suitable phase transi-

tion model which relies on two main assumptions: (i) the dust grain always retains its spherical shape (in particular, the ablation processes are assumed spherically symmetric and there is no "rocket effect"), (ii) the only sources of mass loss considered are the gas phase transitions. Mass loss rate $dM_d/dt$ due to surface evaporation is described via the Hertz-Knudsen formula (HK), which provides the theoretical maximum atomic flux leaving the grain surface [31]:

$$\left(\frac{dM_d}{dt}\right)_{HK} = -\sqrt{\frac{m_{at}}{2\pi R}} \cdot A_d \cdot \frac{p_v\left(T_d\right)}{\sqrt{T_d}} \tag{1}$$

$m_{at}$ and $p_v(T_d)$ are the molar mass and the vapor pressure (as a function of $T_d$) of the dust material, $R$ the gas constant and $A_d$ the area of the dust particle ($4\pi R_d^2$ for spherical dust particles). The mass loss due to gas phase transitions also corresponds to a loss of power, $Q_{gas}$, estimated as the sum of the power that the cloud of gaseous matter had as a part of the dust particle and the power necessary to gasify its mass.

When no bulk phase transition is occurring (the dust particle is entirely solid or liquid), the change of mass of the dust grain is determined only by surface evaporation. During bulk phase transitions instead, dust temperature $T_d$ stops changing as long as the process is not complete and the latent heat of the dust material ($\Delta h_{i\to f}$, with $i$ and $f$ the labels of the initial and final phase, respectively) needs to be taken into account. In this case, the equation for the dust particle enthalpy leads to two equations describing the evolution of the masses of the two phases present.

As some of the other codes do [11,15], to properly evaluate the evolution of $T_d$, the temperature dependence of the various thermodynamic properties (enthalpy, specific heat, vapor pressure, etc.) of dust particles has been effectively introduced in DUSTTRACK by means of suitable polynomial fits of tabulated experimental values [32,33].

### 3.3 The active force module

The active force module, which finally determines the trajectories of the test dust particles, is based on the Newton's equation of motion. It implements the friction forces affecting the dust particles due to the interaction with the plasma species and impurities (because of their small mass, electrons are neglected in the momentum transfer process), generally indicated with $\mathbf{F}_{drag}$, the Lorentz force $\mathbf{F}_{Lorentz} = q_d(\mathbf{E} + \mathbf{v}_d \times \mathbf{B})$ (where $\mathbf{E}$ and $\mathbf{B}$ are the electric and magnetic fields) and the gravitational force $M_d\mathbf{g}$. A distinctive hallmark of DUSTTRACK is the description of the magnetic dipole force $\mathbf{F}_{\nabla\mathbf{B}}$ [14] in case of ferromagnetic dust grains. This situation is not so rare due to the presence of iron and nickel in steel and Inconel commonly used in tokamaks as structural materials. $\mathbf{F}_{\nabla\mathbf{B}}$ is tied through $\nabla\mathbf{B}$ to the magnetic field inhomogeneity, which naturally arises considering the toroidal geometry of tokamaks.

Another contribution to $\nabla \mathbf{B}$ comes from the discretness of the field coils inducing a modulation of $\mathbf{B}$, the so-called "magnetic field ripple" [34]. All these effects are completely modeled by DUSTTRACK.

The drag force due to charged plasma species can be separated in two terms, the first due to their absorption by the dust grain ($\mathbf{F}_{coll}$, collection drag force) and the second due to small-angle Coulomb collisions with closely orbiting plasma particles ($\mathbf{F}_{orb}$, orbital drag force). For neutral plasma species, the latter contribution is clearly not present. Both $\mathbf{F}_{coll}$ and $\mathbf{F}_{orb}$ are calculated following [11]. For the latter, the adopted method of evaluation of Coulomb logarithm is the one proposed by I.H. Hutchinson in [35] and based on the work of S.A. Khrapak et al. [36].

The DUSTTRACK code can indeed cope with any fast time scale related to dust dynamics even in a realistically evolving plasma, should the background plasma profiles be all available. In the range of applications envisaged the plasma (ion) flow in the SOL is laminar (with a small fluid Reynolds number) and effects of turbulence, specifically on the dominant drag force, are not included since no definitive theory exists yet of the various turbulence mechanisms possible in the SOL. The question certainly goes beyond the aims of this work, and it would be unsafe to mock it up in a code whose primary objective is soundness and reliability for application to fully available input data. However, for certain investigations an empirical extension can be performed, through an "effective" collision frequency, proportional to the appropriate turbulence level.

### 3.4 The reflection module

The issue of dust-PFCs interactions is addressed in DUSTTRACK by means of a flexible reflection model. On one hand, some codes in the fusion community, like DTOKS [12,13], completely neglect the dust-wall collisions. This has the consequence of prematurely removing dust particles before complete ablation, underrating their lifetime and length of the trajectories. On the other hand, a full and detailed treatment of reflections is implemented in MIGRAINe [4,15, 16].

DUSTTRACK, as MIGRAINe, models collisions as impulsive forces which lead to a discontinuous change of the particles velocity [15]. This assumption relies on the fact that an appropriate time-scale for dust-wall interactions is on the order of tens of ns [15] and typical DUSTTRACK time-steps are fractions of $\mu$s. In its simplest implementation, DUSTTRACK reflection module describes perfectly elastic mirror-like reflections. In its more comprehensive version, instead, it includes inelastic effects and consideration of PFCs surface roughness through a randomization of the direction vector of the dust particle after the reflection from the vessel.

The inelastic character of the interactions is treated starting from the approach of C. Thornton and Z. Ning [37]. The grain velocity loss after the collision is modeled using suitable normal and tangential restitution coeffi-

cients [38,39,40,41,15]. The normal and tangential components of the reflection velocity ($V_n$ and $V_t$) are:

$$V_n = -e_n v_n \tag{2}$$

$$V_t = v_t - (1 + e_n)\,\mu |v_n| \mathrm{sgn}(v_t) \tag{3}$$

where $v_n$ and $v_t$ are the normal and tangential components of the velocity of the colliding particle, $e_n$ is the normal restitution coefficient ($0 \leq e_n \leq 1$) and $\mu$ the Coulomb friction coefficient ($\mu \geq 0$). A reversal of the reflection tangential velocity occurs if $|v_t| < (1+e_n)\mu|v_n|$. In such a case DUSTTRACK puts $V_t = 0$.

Furthermore, a "sticking" limit was introduced: if the normal reflection velocity of the dust particle is below this value, no rebound occurs. [37,42] point out that the sticking velocity depends on the mechanical properties of the materials involved in the collision, and on the radius of the dust particle. Recent experimental studies of the physics of low speed impacts [16] have improved the understanding of re-bouncing, sticking and sliding/rolling phenomena for dust grains impacting on a target. In this paper, however, the sticking velocity is a constant parameter eventually taken from empirical values.

The issue of PFCs roughness at the $\mu$m-scale, which could strongly modify the geometry of the interactions between dust particles and tokamak vessel, is properly tackled in DUSTTRACK randomly extracting from a cosine distribution the unit direction vector of the dust particle after the collision (this approach is different from that of MIGRAINe [15]). For further details about the algorithm implemented in DUSTTRACK see subsection 5.3.

### 3.5 DUSTTRACK equations

The DUSTTRACK modular structure presented in the previous subsections leads to a set of coupled time ODEs involving, for each particle, a total of 9 parameters: the six phase variables ($x$, $y$, $z$ and $v_x$, $v_y$, $v_z$), the temperature $T_d$, the charge $q_d$ and the mass $M_d$ (eventually two masses in case of bulk phase transitions). The equations for position and velocity of the dust particle C.M. (in Cartesian coordinates) are

$$\frac{d\mathbf{x}_d}{dt} = \mathbf{v}_d \tag{4}$$

$$M_d \frac{d\mathbf{v}_d}{dt} = \mathbf{F}_{darg} + \mathbf{F}_{Lorentz} + M_d\mathbf{g} + \mathbf{F}_{\nabla \mathbf{B}} \tag{5}$$

and the equation for the dust particle charge is

$$\frac{dq_d}{dt} = I_{plasma} + I_{SEE} + I_{TI} \tag{6}$$

Considering the heating module, DUSTTRACK basically activates different equations when one or two phases are present. The labels of "s", "l" and "g"

are used to indicate the solid, liquid and gas phases. Starting with a single phase dust particle, DUSTTRACK solves

$$\frac{dT_d}{dt} = \frac{1}{M_d c_{p,d}} \left( Q_{plasma} + Q_{SEE} + Q_{TI} + Q_{rad} + Q_{gas} \right) \tag{7}$$

with

$$Q_{gas} = \Delta h_{gas} \left( \frac{dM_d}{dt} \right)_{HK} \tag{8}$$

where $\Delta h_{gas}$ is the latent heat associated to the surface evaporation ($\Delta h_{s \to g}$ for solid dust particle and $\Delta h_{l \to g}$ for liquid dust particle). During bulk phase transitions, instead, since the dust temperature maintains constant, $dT_d/dt = 0$. For melting, the equations which govern the process are the ODEs for $M_{d,s}$ and $M_{d,l}$, the solid and liquid mass of the dust grain:

$$\begin{aligned} \frac{dM_{d,s}}{dt} &= -\frac{Q_{tot}}{\Delta h_{s \to l}} \\ \frac{dM_{d,l}}{dt} &= \frac{Q_{tot}}{\Delta h_{s \to l}} + \left( \frac{dM_{d,l}}{dt} \right)_{HK} \end{aligned} \tag{9}$$

To avoid numerical errors, the transition is considered over when the radius of the inner phase $R_{d,s}$ is below 20 nm. The associated critical value for the mass of the solid phase is evaluated using $M_{d,s} = 4/3\pi\rho R_{d,s}^3$, where $\rho$ is the density of the material of the dust particle. Finally, for boiling (or sublimation), since the gasified mass is considered lost, DUSTTRACK solves a single equation for the evolution of the mass of the inner phase $M_{d,l}$ (or $M_{d,s}$ for sublimation)

$$\frac{dM_{d,l(s)}}{dt} = -\frac{Q_{tot}}{\Delta h_{l \to g(s \to g)}} + \left( \frac{dM_{d,l(s)}}{dt} \right)_{HK} \tag{10}$$

With the purposes of avoiding round-off errors due to manipulation of small and large numbers and eventually assessing the relative importance of the different terms in the model equations, DUSTTRACK actually considers a dimensionless form of the set of ODEs described so far. The dimensionless quantities $\overline{q}_d$, $\overline{M}_d$, $\overline{T}_d$, $\overline{\mathbf{x}}_d$, $\overline{\mathbf{v}}_d$ for dust charge, mass, temperature, position, velocity, $\overline{\mathbf{B}}$ and $\overline{\mathbf{E}}$ for the magnetic and electric fields and $t_0$ for the time $t$, are introduced. They are defined through the following characteristic parameters: the elementary charge $e$, the initial mass and velocity of the dust particle $M_{d,i}$ and $|\mathbf{v}_{d,i}|$, the melting (or sublimation) temperature of the material of the dust particle $T_{s \to l(s \to g)}$, reference length $L_0 = 1$ m and magnetic field $B_0 = 1$ T. Finally, DUSTTRACK dimensional relationships are:

$$\begin{aligned} &\overline{q}_d = q_d/e && \overline{M}_d = M_d/M_{d,i} && \overline{T}_d = T_d/T_{s \to l(s \to g)} \\ &\overline{\mathbf{x}}_d = \mathbf{x}_d/L_0 && \overline{\mathbf{B}} = \mathbf{B}/B_0 && t_0 = tB_0 e/M_{d,i} \\ &\overline{\mathbf{v}}_d = \overline{\mathbf{x}}_d/t_0 && \overline{\mathbf{E}} = \mathbf{E}/\left( |\mathbf{v}_{d,i}| \, B_0 \right) \end{aligned}$$

Once the apparatus of equations to investigate the dynamics of dust particles in tokamaks is set up, it is necessary to define thorough conditions for

the termination of their life. There are two of them in the current version of DUSTTRACK: (i) the grain completely ablates, (ii) the grain sticks to one of the tokamak PFCs. Since several effects, e.g. field emission, not modeled in the code are expected to play a role when $R_d$ falls below some tens of nm, a $M_d$ value corresponding to a radius of 20 nm is adopted as the critical mass for the termination of the dust particle trajectory.

## 4 DUSTTRACK input data

The complexity of the topic of dust dynamics in tokamaks reflects also on the input information of simulation codes. Primarily, the dust particles material and thermodynamic properties (see subsection 3.2) have to be provided to DUSTTRACK. Secondly, its computational domain needs to be defined by a detailed geometry of tokamak chamber and PFCs. Thirdly, the profiles of the magnetic and electric fields have to be specified, as well as those of the main ambient plasma parameters (section 2). Lastly, DUSTTRACK asks for the initial conditions at time $t_i$ of the test dust particles, namely their starting mass, temperature, charge, position and velocity.

The access to experimental data of magnetic, plasma and vessel profiles is done via a tokamak dependent Fortran 90 routine which maps the database variables onto the DUSTTRACK data structure. The information of magnetic and electric fields is typically written in a EQDSK format file [18] which also contains the details of the PFCs geometry, in the form of a 2D (3D) closed polygon (surface). The latter is read in by the code, in Cartesian coordinates and used in the dynamics calculations to account for dust particles reflections. Ambient plasma profiles are read from text files provided after runs of the SOL transport code EDGE2D [19, 20] (or equivalent). It gives the 2D (axisymmetric) cross-section profiles of densities, temperatures and velocities of the different plasma species and impurities. Since the meshes of EDGE2D do not extend till the tokamak chamber and core, the resulting plasma profiles refer to a "belt" region across the separatrix and the SOL layer. However, the volume externally the SOL is the region where dust particles can spend most of their life and PFCs not intersecting the magnetic field lines can anyway constitute places for dust accumulation. Some numerical extrapolation of the plasma profiles to the vessel is therefore necessary but not always implemented in the dust codes of the tokamak community (e.g. DTOKS). The technique currently used in DUSTTRACK is a form of the inverse distance weighting Shepard's method [43], where exponential weighting functions with a proper decay length (which depends on specific plasma collisionality and parameters at LCMS [44]) are chosen. This method has the advantage of simplicity, and is suitable to work with scattered data on any grid, even though it has some negative features, like the tendency to give excessive weight to outliers. An example of the output of this extrapolation procedure is shown in figure 1b.

## 5 Description of the DUSTTRACK architecture

DUSTTRACK is written in Fortran 90. It takes advantage of Fortran 90 user-defined data types, dynamic memory allocation and module units. The code consists of three parts: the preprocessing module which reads the input data and initializes the DUSTTRACK variables, the solution block which solves the ODEs system of subsection 3.5 through the solver DASKR (Differential-Algebraic Solver with Krylov methods and Root-finding) [45] and the postprocessing part that stores or plots the solutions of the system. The flow diagram of figure 2 shows a condensed view of the working scheme of DUSTTRACK. The pre- and postprocessing modules have a straightforward and sequential structure and they are not described here. The solution block, which is the more critical part, comprises: the DASKR software, the subroutines necessary for the interface between DUSTTRACK and DASKR and the algorithms to handle the constraint conditions on the dust particles properties. Each component of the solution block will be presented within this section in detail.

### 5.1 Solution block: general structure

As anticipated in section 3, in DUSTTRACK the dust-dust interactions are neglected and the system of equations describing the evolution of the $D$ time-dependent quantities ($D$ = six phase variables plus dust particles physical parameters, e.g. $D$=9 in this work, see subsection 3.5) of a collection of $N$ particles consists of $D$ coupled ODEs for each particle for a total of $D\times N$ ODEs. Considering a single particle, generally labeled with the index $J$ in the following, the $D$ unknown parameters are stored as elements of the array $\mathbf{p}_J$ according to the following order:

$$\mathbf{p}_J = (\overline{x}_d, \overline{v}_{d,x}, \overline{y}_d, \overline{v}_{d,y}, \overline{z}_d, \overline{v}_{d,z}, \overline{q}_d, \overline{T}_d, \overline{M}_d)_J \tag{11}$$

When a bulk phase transition is occurring, $\overline{M}_d$ is the mass of the inner phase (e.g. "solid" during melting) and $\overline{T}_d$, whose value maintains constant, is replaced with the mass of the outer phase. The $N$ arrays $\mathbf{p}_J$ are allocated by DUSTTRACK as column vectors in the matrix $\mathbf{P}$: the matrix of the unknown variables. Its dimensions are clearly $D\times N$.

Unlike other codes, DUSTTRACK was conceived to follow simultaneously the dynamic evolution of a multitude of particles and not just one at a time. Beside this, the $D$ equations for the dust parameters involve widely different time scales which make the ODEs system stiff. Moreover, the latter is also connected to constraint functions where some boundaries define the end of the integration for the particles (e.g. the vessel contour) and may be followed by a restart of the time integration with new calculated initial conditions (in case of reflections). A careful and competent selection for the most reliable ODEs solver was accordingly needed, warranting robustness and efficiency in the calculations. The choice of the software package for the integration of the $D\times N$

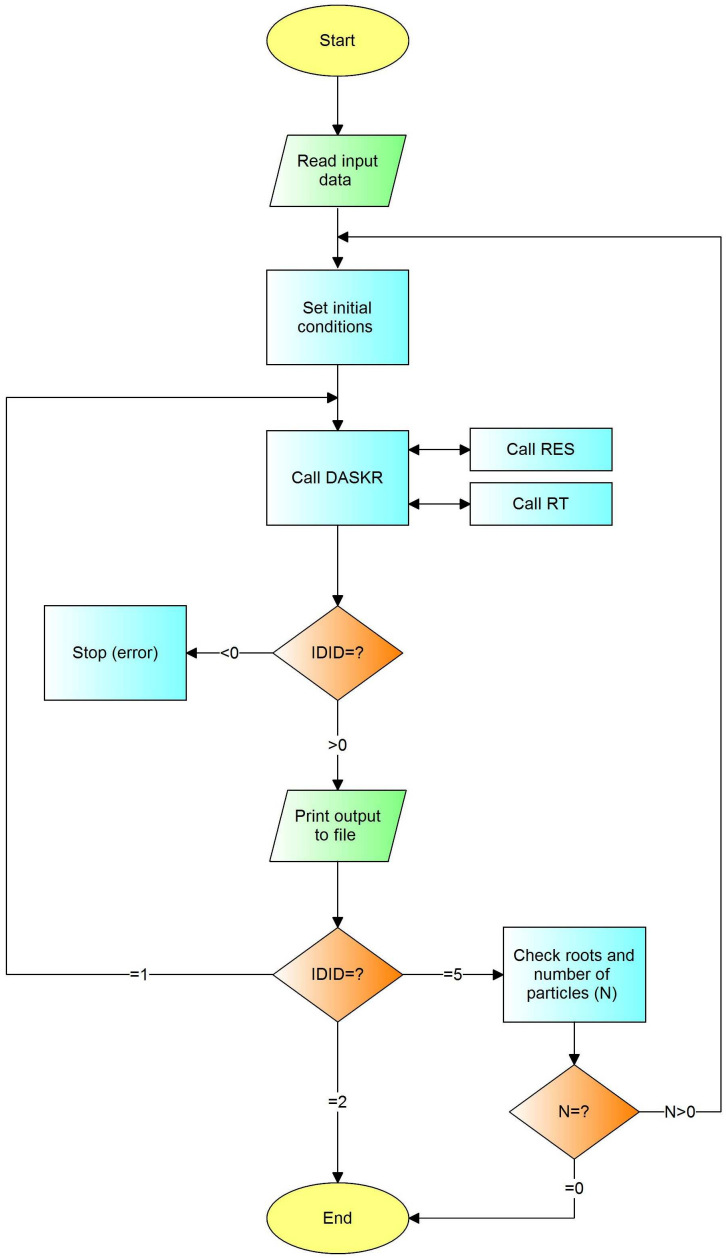


**Fig. 2** The flow diagram describing the working scheme of DUSTTRACK.

ODEs came down to DASPK (Differential-Algebraic Solver Preconditioned Krylov) [45], which satisfies all these requirements. It is an evolution of the popular DASSL code (Differential-Algebraic System SoLver) [46]. DASPK uses variable-order and variable-stepsize backward differentiation formulas that are particular appropriate for the solution of stiff problems where the characteristic times related to the differential equations can vary over order of magnitude. Within the DASPK software package, the Fortran 77 routine DASKR was chosen because it includes a root-finding algorithm which permits to find the roots of a given set of constraint functions while the integration of the system is performed (subsection 5.2).

Actually, DASKR generally solves systems of Differential-Algebraic Equations (DAEs) of the form $G(t,\mathbf{Y},\dot{\mathbf{Y}})=0$, where $\mathbf{Y}$ and $\dot{\mathbf{Y}}$ are vectors. $\mathbf{Y}$, the array of the unknown variables, is referred as "solution vector" in the following. $\dot{\mathbf{Y}}=d\mathbf{Y}/dt$ is the time derivative of $\mathbf{Y}$. The software DASKR is designed in such a way that the user writes an interface subroutine "RES" in which, given the $\mathbf{Y}$ and $\dot{\mathbf{Y}}$ vectors at time $t$, $G(t,\mathbf{Y},\dot{\mathbf{Y}})$, or "residual", is computed. At the starting time $t_i$, the initial values for $\mathbf{Y}$ and $\dot{\mathbf{Y}}$ must be given as input to DASKR. DASKR solves the system under investigation from $t_i$ to a specified $t_{stop}$. In the frame of this work, $t_{stop}$ coincides with the duration of the plasma pulse. Moreover, the DASKR automatic selection option of the time-steps ($\Delta t$) has been chosen in order to achieve the desired accuracy of the solution of the system with the least computational effort. Due to the severe scaling difficulties of DASKR during the first time-steps, every time the DAEs solver restarts with new initial conditions, $\Delta t \simeq 10^{-10}$ s is set.

While integrating the system, DASKR also searches for roots of the constraint functions $R_i(t,\mathbf{Y},\dot{\mathbf{Y}})$, which are defined by the user through the subroutine "RT". If DASKR finds a sign change in any $R_i(t,\mathbf{Y},\dot{\mathbf{Y}})$, it returns the intermediate values of $t$ and $\mathbf{Y}$ for which $R_i(t,\mathbf{Y},\dot{\mathbf{Y}})=0$.

As discussed above, DASKR works with vectors as input. By contrast, DUSTTRACK manages the matrixes $\mathbf{P}$ and $\dot{\mathbf{P}}=d\mathbf{P}/dt$. Inside the DUSTTRACK program unit, these two matrixes are suitably transformed into the $\mathbf{Y}$ and $\dot{\mathbf{Y}}$ arrays in order to be processed by the DASKR subroutine.

### 5.2 Solution block: interface between DUSTTRACK and DASKR

After each $\Delta t$, DUSTTRACK interfaces to DASKR through the two aforementioned user-supplied subroutines RES and RT. RES takes as input the current time $t$, the matrixes $\mathbf{P}$ and its time derivative $\dot{\mathbf{P}}$ and produces the residual of the ODEs system: $G(t,\mathbf{P},\dot{\mathbf{P}})$. As an intermediate step, RES obtains/computes the following quantities:

- electric and magnetic vectors, $\mathbf{E}$ and $\mathbf{B}$, at the dust particle position $(x_d, y_d, z_d)_J$, read from the EQDSK file.
- temperature, density and velocity of electrons, ions and neutrals of the background plasma, at the dust particle position $(x_d, y_d, z_d)_J$, by extrapolating the EDGE2D profiles.

– net force acting on the dust particle.
– net electric current to the dust particle.
– net heat flux to the dust particle.

Moving on to the subroutine RT, it is written to define the vector of constraint functions, whose roots are searched for during the time integration performed by DASKR. As the subroutine RES, RT asks for the time $t$ and the matrixes $\mathbf{P}$ and $\dot{\mathbf{P}}$. It gives as output the array "**RVAL**", whose $k$-th element is the value of the constraint function $\mathrm{R}_k$ at $(t,\mathbf{P},\dot{\mathbf{P}})$: $\mathbf{RVAL}(k)=\mathrm{R}_k(t,\mathbf{P},\dot{\mathbf{P}})$. The problem of investigating the dust particles trajectories in tokamaks, as modeled by DUSTTRACK, imposes two kinds of constraint: the geometric contour of the vacuum vessel and the physical constraints. In particular, the former delimits the physical domain of the simulations and when it is reached by some dust particles leads to an abruptly change of their velocity (due to the reflection from or adhesion to PFCs). The latter consist in some physics conditions that if satisfied can bring to the substitution of some equations in the system $\mathrm{G}(t,\mathbf{P},\dot{\mathbf{P}})$ (when a bulk phase transition begins) or to the end of the story of the dust particle (when its mass is approximately zero). It follows that, the physical constraints are the temperatures at which the bulk phase transitions occur and the critical value for the radius of the dust particle, $R_d = 20$ nm. In these cases, the typical form of the $k$-th constraint function associated to the I-th parameter and the J-th dust particle is:

$$R_k = \mathbf{P}(I,J) - \mathbf{P}_b(k) \tag{12}$$

where $\mathbf{P}_b(k)$ is one of the values of the physical constraints introduced so far (for example the melting temperature).

Considering the vacuum vessel contour, it is represented by a manifold of straight lines (eventually planar surfaces) to form a closed 2D polygon (3D surface) and generally has a concave shape. In order to know when the dust particles-PFCs interactions happen, the modeling issue of determining whether or not a point of the trajectory of a given dust particle lies in- or outside the vessel contour has to be considered. One of the commonly used algorithms to face this problem in 2D is that suggested by S. Nordbeck and B. Rystedt in [47]. The improved version of S.W. Sloan is implemented in DUSTTRACK using the Fortran 77 subroutine "PINPOL" (acronym of Point-IN-POLygon), which is reported in Appendix 1 of [48]. In detail, PINPOL returns the variable "MINDST" which contains the distance between the position of the particle and the nearest point on the vessel polygon. If MINDST is positive (negative), the particle is inside (outside) the vessel. During integration, the DASKR solver searches for the roots of MINDST. In particular, a root is detected whenever MINDST changes sign. In this case, MINDST$\simeq$0 and the particle has impinged on a side of the polygon and can be reflected from or stuck to the vessel.

### 5.3 Solution block: DASKR flag IDID

Coming back to the structure of the DASKR software, after each time-step, together with the solution of the system G and its time derivative, DASKR returns the flag variable "IDID", which reports the status of the calculation (see also the flow diagram of figure 2). A negative value of IDID means that an error was encountered and information on the possible cause is provided. If IDID>0 the time-step was successfully taken. In particular, IDID=1 means that the current time is different from the final time $t_{stop}$ and DASKR is preparing for the next time-step. If IDID=2, instead, $t_{stop}$ has been successfully reached. When IDID=5 one or more roots of the given constraint functions $R_i$ have been found. In this case, DASKR specifies also which of the $R_i$ have a root and DUSTTRACK detects then the dust particles associated to these functions $R_i$. Once one of the roots is obtained, DUSTTRACK acts in different ways depending on the nature of the constraint which has been satisfied.

Considering first the physical constraints, if one of the phase transition temperatures has been reached for particle $J$: (i) DASKR is restarted taking account of the substitution in $\mathbf{p}_J$ of the quantity $\overline{T}_d$ with the non-dimensional mass of the outer phase, (ii) the ODEs in RES are automatically updated to suitably model the phase transition and (iii) in RT the vector of the constraints, $\mathbf{P}_b$, changes accordingly. For example, when $T_d$ is equal to the melting temperature and the associated bulk phase transition starts, the equation 7 for the time derivative of $T_d$ is replaced in RES with the two equations 9 for the evolution of the solid and liquid mass, $M_{d,s}$ and $M_{d,l}$, of the dust particle. The physical constraint of melting which, when reached, indicates the end of the phase transition (the particle becomes completely liquid) is the critical mass of the inner solid phase (see subsection 3.5). The latter replaces the melting temperature in the array $\mathbf{P}_b$.

In case that, instead, for whatever reason (surface evaporation, sublimation or boiling), the thermodynamic mass loss brings the external radius $R_d$ of one or more dust particles below the critical value of 20 nm, they are regarded to their end of life and the DASKR software no longer considers the corresponding $\mathbf{p}_J$ vectors.

Moving on to the other type of constraint: the vacuum vessel, a reflection algorithm is applied every time a dust particle hits one side of the vessel contour. At the time-step following the reflection, the DASKR restarts with the new values of the velocity components of the dust particle. As presented in subsection 3.4, DUSTTRACK offers different options for the evaluation of the direction and speed of the particle after the collision. In particular, in order to describe the effect of the vessel micrometer roughness on the dust particles trajectories, the hypothesis made is that the reflection unit direction vector is distributed according to a cosine distribution [49]. In DUSTTRACK a very simple algorithm is used to extract the unit reflection vector from a cosine distribution. The sampling method is based on the fact that the sum of the unit direction vector of the impinging particle and a unit random vector, uniformly distributed over a sphere, follows a cosine distribution. The desired

random unit direction vector after the collision is therefore directly obtained from a spherically distributed unit vector. Both the details of this approach and the syntax of the algorithm implemented in DUSTTRACK are described in [49] and references therein.

Moreover, when the dust particles-vessel interactions are considered inelastic, normal and tangential restitution coefficients and the concept of a sticking velocity are introduced to model the dust particle velocity after the collision (see subsection 3.4). In the case that the normal component of the reflection velocity is below the sticking velocity, the dust particle is considered stuck at the surface of the vessel and the corresponding $\mathbf{p}_J$ is excluded from the ODEs resolution process.

### 5.4 Solution block: update of the number of dust particles

Since the number of ODEs which DUSTTRACK has to solve, $D \times N$, rapidly increases with the number of dust particles, the wise handling of the memory space to remove from the ensemble the particles which have reached, before others, their end of life (i.e. by mass reduction to a chosen lower limit or when the normal reflection velocity of the dust particle is below the sticking velocity), as well as the strategies adopted to reduce the calculation time in DASKR, become crucial aspects.

Foremost, every time a dust particle reaches its end, the corresponding $\mathbf{p}_J$ vector is deleted from the DAEs system. The matrixes $\mathbf{P}$ and $\dot{\mathbf{P}}$ are rearranged in such a way that the $\mathbf{p}_J$ associated to the death particle is moved to the final column of the matrixes, while shifting all the other columns one position to the left. This operation is called circular shift and it is performed in Fortran 90 through the arrays manipulation function "CSHIFT".

The DASKR software acts on the Jacobian matrix of the system $\mathrm{G}(t,\mathbf{P},\dot{\mathbf{P}})$ to find the solution. The Jacobian is the matrix whose elements are the partial derivatives of the ODEs of the system with respect to the components of the $\mathbf{p}_J$ arrays of all the particles. From a computational point of view, the DASKR software works faster with band Jacobian matrixes. It follows that, a way to save calculation time and complexity consists in minimizing the bandwidth of the Jacobian matrix of the system G. It has been demonstrated that the bandwidth of the Jacobian of G is given by the number of rows of the matrix $\mathbf{P}$. This is the reason why $\mathbf{P}$ (whose size is $D \times N$) is built in such a way that the $\mathbf{p}_J$ arrays are arranged in columns instead of rows otherwise leading to a matrix size of $N \times D$, where $N$ is typically greater than $D$ (at least at the beginning of the simulation).

## 6 Typical output of DUSTTRACK

Among the possible applications, DUSTTRACK has been used to predict the trajectories of heavy metals dust particles produced in the tokamak JET, to

assess their mobilization from the surface of the PFCs, their final deposition and the effects of collisions with the PFCs as well as the monitoring of the penetration of particulate in the SOL closer to the separatrix which causes plasma contamination through dust ablation. The results should allow some indirect crosscheck with existing diagnostics such as impurity spectroscopy, fast camera tracers and high resolution Thomson scattering techniques [5,6, 7]. In this section, some representative results obtained in the frame of this activity by DUSTTRACK are described in order to show a possible realistic output of the code.

Presently JET is characterized by bulk Be, Be coated inconel or W coated Carbon Fibre Composite (CFC) PFCs in the main chamber wall and W coated CFC with one row of bulk W in the divertor [50]. For experimental reasons related to the understanding of Transient Impurity Events (TIEs) [5,6,7], DUSTTRACK was applied to investigate the dynamics of W spherical dust particles with 10 $\mu$m-radius produced from JET divertor region. The background plasma was taken from an EDGE2D simulation of JET pulse #82806 at 55-56 s (figure 1). To study the 3D transport of dust, the plasma, as well as the JET vessel, were supposed axisymmetric. A bunch of several (>10) W particles was launched both from the inner and the outer divertor (see figure 1a), with an initial speed $|\mathbf{v}_{d,i}|$ of 10 m/s and different input angles. Ambient plasma and dust particles main parameters are summarized in table 1. The comprehensive version of DUSTTRACK reflection module (i.e. inelastic collisions and consideration of PFCs surface roughness through a randomization of the direction vector of the dust particle after the reflection from the vessel, subsections 3.4 and 5.3), with an artificial sticking velocity of 1 m/s, is used.

**Table 1** Some of the input parameters of DUSTTRACK for JET shot #82806 at 55-56 s. $T_{e(i),sep}$ and $n_{e(i),sep}$ are plasma electron (ion) temperature and density on the separatrix at the outer midplane, respectively. $R_{d,i}$ and $T_{d,i}$ are the initial radius and temperature of the tungsten dust particles which were launched with initial velocity $|\mathbf{v}_{d,i}|$ and different input angles from JET divertor.

| $T_{e,sep}$ | $T_{i,sep}$ | $n_{e,sep} = n_{i,sep}$ | $R_{d,i}$ | $T_{d,i}$ | $\lvert\mathbf{v}_{d,i}\rvert$ |
|---|---|---|---|---|---|
| 387 eV | $T_{e,sep}\times 1.6$ | $0.948\times 10^{19}$ m$^{-3}$ | 10 $\mu$m | 300 K | 10 m/s |

DUSTTRACK constraints (subsection 5.2) sort test dust particles, depending on the termination condition which they encounter during the simulation, in stuck and ablated. The former are relevant for re-deposition studies and the latter for plasma contamination. In case of tungsten, the ablation channels are surface evaporation and boiling. In principle, W dust particles can completely ablate through surface evaporation before the boiling temperature is reached. It follows that three representative cases can be identified:

#1 Dust particle finally sticks to some PFCs.
#2 Dust particle entirely ablates through surface evaporation.
#3 Dust particle entirely ablates through surface evaporation and boiling.

Among all the simulations performed, DUSTTRACK results relative to one dust particle for each of the above categories are shown. The missing initial conditions of the selected particles are reported in table 2. Figure 3 depicts the

**Table 2** Starting position, input angle (measured, considering figure 3, from the axis $r = \sqrt{x^2 + y^2}$, counterclockwise) and destiny of the simulated dust particles launched from JET divertor region, for shot #82806 at 55-56 s. $y_{d,i}$ is the same for all the three particles.

| Particle | $x_{d,i}$ | $z_{d,i}$ | $\theta_{d,i}$ | Fate |
|---|---|---|---|---|
| #1 | 2.44 m | -1.69 m | 20° | Adhesion |
| #2 | 2.86 m | -1.71 m | 120° | Evaporation |
| #3 | 2.86 m | -1.71 m | 80° | Boiling |

trajectories of the three dust particles, within the JET poloidal cross-section, as computed by DUSTTRACK. The contour of the JET divertor and the LCMS are also displayed. The evolution of the dust particles physical parame-

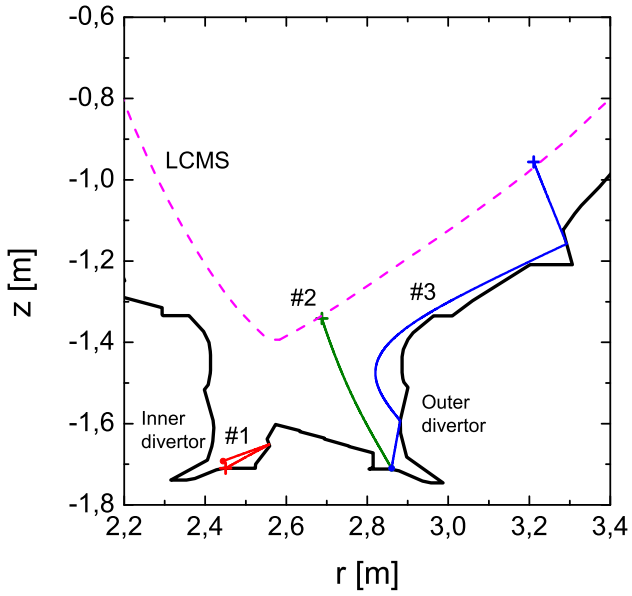


**Fig. 3** Trajectories of 10 $\mu$m-radius W dust particles, with initial speed of 10 m/s launched from JET divertor, as predicted by DUSTTRACK. The starting and final points are labeled with a full circle (•) and a plus sign (+), respectively.

ters: module of velocity $|\mathbf{v}_d|$, normalized electric potential $\chi_d$ ($= -e\phi_d k_B^{-1} T_e^{-1}$, where $k_B$ is the Boltzmann constant), temperature $T_d$ and radius $R_d$, is shown in figure 4. From both figures 3 and 4, it is evident that dust dynamics is strongly influenced by the initial conditions. Particle #1 experiences two in-

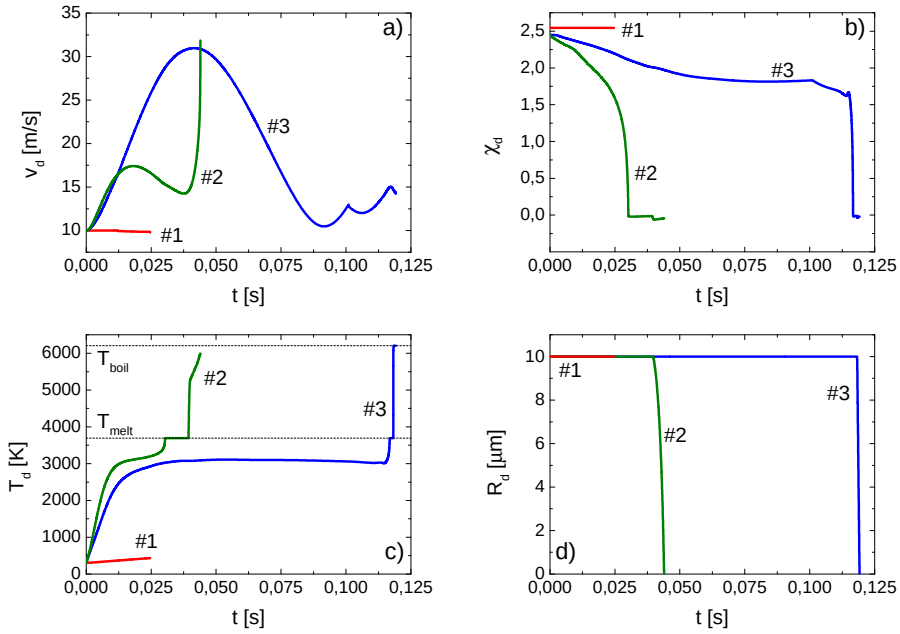


**Fig. 4** Evolution of velocity $|\mathbf{v}_d|$ (a), normalized potential $\chi_d$ (b), temperature $T_d$ (c) and radius $R_d$ (d) of test W dust particles ($R_{d,i}$= 10 $\mu$m), launched with initial speed of 10 m/s from JET divertor, as predicted by DUSTTRACK.

teraction events with the PFCs. Since no significant decrease of the module of velocity occurs ($|\mathbf{v}_d| \simeq |\mathbf{v}_{d,i}|$, see figure 4a), the first collision simply randomizes the direction vector of the dust particle which rebounds toward the starting point finally impinging on the vessel with a local component of the normal reflection velocity below the sticking value of 1 m/s. The motion of particle #1 is limited to the divertor region. Due to the low plasma temperature and density there, dust-plasma interaction is relatively weak and dust particle physical parameters of figure 4 remain nearly unchanged. The trajectory of particle #2 does not intersect the vessel as $\mathbf{v}_{d,i}$ points toward the center of the machine. The more extreme conditions approaching the LCMS (see the profile of the electron temperature of figure 1b) lead to a fast melt of the particle (at $T_{W,melt} = 3695$ K) and to its complete evaporation before the boiling temperature ($T_{W,boil} = 6203$ K) is reached (figure 4c). Melting corresponds to the plateau region of $T_d(t)$ at $T_{W,melt}$ ($dT_d/dt = 0$ during bulk phase transitions). Because $T_d < T_{W,boil}$, surface evaporation constitutes the only channel of mass loss and, as expected from equation 1 and reference [33] (tungsten vapor pressure strongly increases with temperature), becomes important for $T_d > T_{W,melt}$ causing a fast decrease of $R_d$ (figure 4d). Finally, particle #3 scrapes all the outer divertor, colliding twice with some PFCs before diving into the hot plasma. When it travels grazing the wall, hence in the "relatively"

cool and rarefied plasma volume outside the SOL, $T_d$ stays well below $T_{W,melt}$ (figure 4c) and surface evaporation is almost not active at all. Dust mass loss starts when the particle heads toward the plasma core after the second interaction with the chamber, quickly ablating through surface evaporation first and boiling then. The initial conditions of particles #2 and #3 lead to very different trajectories and $T_d$ evolution which ultimately reflect on their lifetime in the tokamak. Particle #2 survives much less than particle #3. Considering figure 4b, it is clear instead that the story of these two particles does not affect the qualitative behavior of their normalized potential $\chi_d$ which maintains almost always positive ($q_d < 0$), and is subject to a sharp decrease concurrently to the likewise stiff increase of $T_d$ occurring when the particles escape from the divertor volume to the high $T_e$ regions. Higher plasma and dust temperatures bring respectively to a growing importance of the SEE and TI emission terms in the dust charging equation 6 with respect to the dominant electron collection current relevant for low $T_d$, thus increasing the incoming positive current and the dust electric potential (see subsection 3.1). Anyway, the corrective factors in the expressions for $I_{SEE}$ [29] and $I_{TI}$ [26] weakly shield the dust grain potential which is limited around zero and does not diverge for the highest values of $T_d$.

## 7 Conclusions

An efficient particles tracking code, DUSTTRACK, has been developed to allow studies and simulation of isolated dust particles dynamics in the SOL of tokamaks. Its structure permits portability on any platform and easy linking with (processed) experimental data.

Although several papers have been published about dust modeling in tokamaks, this work is one of the first in its genre. It focuses not only on the physical model of DUSTTRACK but also goes into details concerning computational and numerical aspects. This technical approach could be worth sharing with other competent developers.

Among the other codes developed within the tokamak community, DUSTTRACK has the peculiar capability of simultaneously determining the 3D trajectories of a multitude of dust particles inside a plasma environment typical of a tokamak device, with a geometrically complicated boundary, giving also a description of thermodynamic phase transitions, mass variation by ablation and charging processes, which involve widely different time scales, that make the ODEs system to be solved stiff. In fact, the dynamics of a dust particle is described not only by the traditional Newton's equations of motion (six equations) but by additional equations for the evolution of further degrees of freedom and state variables of the particle. These equations are expressed as a balance between input and output fluxes to the dust particle, describing the evolution of the dust charge, temperature and mass. In total DUSTTRACK deals with 9 nonlinear coupled equations for each particle. Furthermore these equations are connected to constraint functions where some boundaries define

the end of the integration for that particle and may be followed by a restart of the time integration with new calculated initial conditions.

The use of Cartesian coordinates, albeit an apparently simple choice, has the property of easy performance for any device, tokamaks or stellarators, even with 3D vessel geometry, and has a safer numerical implementation. This aspect distinguishes DUSTTRACK from the other codes which typically rely on a cylindrical or toroidal reference system very suitable for the description of the simpler geometry of tokamaks with circular cross section.

A careful and competent choice was needed for the most reliable ODEs solver suitable for the problem, warranting robustness and efficiency in the calculations. An important aspect of the code is the wise handling of the memory space to remove from the ensemble the particles which have reached, before others, their "end of life" (e.g. by mass reduction to a chosen lower limit or when the normal reflection velocity of the dust particle is below the sticking velocity).

Also important and not trivial although, merely technical, is the I/O organization suitable to study dust dynamics in any toroidal device, from experimental data when available, or from model data for self tests and predictive studies. The background magnetic and plasma profiles are read in from experimental databases or by test-mode files through routines performing the mapping and necessary extrapolation from the original database mesh to the Cartesian working space mesh.

The comparison with another well-established tokamak dust simulation code, DTOKS [12,13], has been performed and published in [17], and the results give confidence that DUSTTRACK is a suitable tool for in depth studies of dust mobilization, interaction with PFCs and plasma contamination. An indirect cross-check of DUSTTRACK predicted dust trajectories and parameters with real tokamaks data from existing diagnostics should finally highlight the correlation between dust dynamics and tokamaks performance.

The wide range of physical processes and plasma environments involved in tokamak dust dynamics stresses the possible incompleteness of the aforementioned DUSTTRACK physics model. Some of the processes which have been ignored up to now and can potentially affect the behavior of dust particles are: the shield effect of dust particles ablating cloud on the incoming plasma particles fluxes, the dust grains rotation due to asymmetric evaporation and the effect of the plasma drag force on the motion of the C.M. of melting dust particles. Another issue is the evaluation of the impact of non-spherical dust morphology on dust particles dynamics. Once the basic equations underlining some of these phenomena will be identified, the modular structure of DUSTTRACK permits an easy and straightforward update of its physics model.

**Acknowledgements** This work has been carried out at the Istituto di Fisica del Plasma IFP-CNR. The views and opinions expressed herein do not necessarily respect those of IFP-CNR.

## References


1. G. Federici, H. Wuerz, G. Janeschitz, R. Tivey, Fusion Eng. Des. **61–62**, 81 (2002)
2. J.P. Sharpe, D.A. Petti, H.-W. Bartels, Fusion Eng. Des. **63–64**, 153 (2002)
3. S.I. Krasheninnikov, R.D. Smirnov, D.L. Rudakov, Plasma Phys. Contr. F. **53**(8), 083001 (2011)
4. S. Ratynskaia, L. Vignitchouk, P. Tolias, I. Bykov, H. Bergsåker, A. Litnovsky, N. den Harder, E. Lazzaro, Nucl. Fusion **53**(12), 123002 (2013)
5. M. Sertoli, J.C. Flannegan, A. Cackett, E. Hodille, P. de Vries, I.H. Coffey, B. Sieglin, S. Marsen, S. Brezinsek, G.F. Matthews, J.W. Coenen and JET-EFDA Contributors, Phys. Scripta **T159**, 014014 (2014)
6. M. Sertoli, J.C. Flanagan, M. Bacharis, O. Kardaun, A. Jarvinen, G.F. Matthews, S. Brezinsek, D. Harting, A. Cackett, E. Hodille, I.H. Coffey, E. Lazzaro, T. Pütterich, J. Nucl. Mater. **463**, 837 (2015)
7. J.C. Flanagan, M. Sertoli, M. Bacharis, G.F. Matthews, P.C. de Vries, A. Widdowson, I.H. Coffey, G. Arnoux, B. Sieglin, S. Brezinsek, J.W. Coenen, S. Marsen, T. Craciunescu, A. Murari, D. Harting, A. Cackett, E. Hodille, Plasma Phys. Contr. F. **57**(1), 014037 (2015)
8. S.J. Piet, A. Costley, G. Federici, F. Heckendorn, R. Little, in *Fusion Engineering, 1997. 17th IEEE/NPSS Symposium,* vol. 1. pp. 167–170
9. V. Rohde, M. Balden, T. Lunt and the ASDEX Upgrade Team, Phys. Scripta **T138**, 014024 (2009)
10. A.Yu. Pigarov, S.I. Krasheninnikov, T.K. Soboleva and T.D. Rognlien, Phys. Plasmas **12**(12), 122508 (2005)
11. R.D. Smirnov, A.Yu. Pigarov, M. Rosenberg, S.I. Krasheninnikov, D.A. Mendis, Plasma Phys. Contr. F. **49**(4), 347 (2007)
12. M. Bacharis, M. Coppins, J.E. Allen, Phys. Rev. E **82**, 026403 (2010)
13. M. Bacharis, M. Coppins, J.E. Allen, Phys. Plasmas **17**(4), 042505 (2010)
14. E. Lazzaro, I. Proverbio, F. Nespoli, S. Ratynskaia, C. Castaldo, U. deAngelis, M. DeAngeli, J.-P. Banon, L. Vignitchouk, Plasma Phys. Contr. F. **54**(12), 124043 (2012)
15. L. Vignitchouk, P. Tolias, S. Ratynskaia, Plasma Phys. Contr. F. **56**(9), 095005 (2014)
16. S. Ratynskaia, P. Tolias, A. Shalpegin, L. Vignitchouk, M. De Angeli, I. Bykov, K. Bystrov, S. Bardin, F. Brochard, D. Ripamonti, N. den Harder, G. De Temmerman, J. Nucl. Mater. **463**, 877 (2015)
17. A. Uccello, G. Gervasini, F. Ghezzi, E. Lazzaro, M. Bacharis, J. Flanagan, G. Matthews, A. Järvinen, M. Sertoli and JET Contributors, Phys. Plasmas **23**, 102506 (2016)
18. EQDSK Format: `https://fusion.gat.com/theory/efitgeqdsk`
19. R. Simonini, G. Corrigan, G. Radford, J. Spence, A. Taroni, Contrib. Plasm. Phys. **34**(2–3), 368 (1994)
20. A.E. Jaervinen, M. Groth, M. Airila, P. Belo, M. Beurskens, S. Brezinsek, M. Clever, G. Corrigan, S. Devaux, P. Drewelow, T. Eich, C. Giroud, D. Harting, A. Huber, S. Jachmich, K. Lawson, B. Lipschultz, G. Maddison, C. Maggi, T. Makkonen, C. Marchetto, S. Marsen, G.F. Matthews, A.G. Meigs, D. Moulton, M.F. Stamp, S. Wiesen, M. Wischmeier and JET-EFDA collaborators, J. Nucl. Mater. **463**, 135 (2015)
21. P. Stangeby, *The plasma Boundary of Magnetic Fusion Devices* (Taylor & Francis Group, New York, 2000)
22. A. Baron-Wiechec, E. Fortuna-Zaleśna, J. Grzonka, M. Rubel, A. Widdowson, C. Ayres, J.P. Coad, C. Hardie, K. Heinola, G.F. Matthews, Nucl. Fusion **55**(11), 113033 (2015)
23. J.E. Allen, Phys. Scripta **45**(5), 497 (1992)
24. P.K. Shukla, A.A. Mamun, *Introduction to Dusty Plasma Physics.* Series in Plasma Physics and Fluid Dynamics (CRC Press, 2001)
25. S. Dushman, Rev. Mod. Phys. **2**, 381 (1930)
26. A.H.W. Beck, *Thermionic Valves* (Cambridge University Press, 2015)
27. R.A. Langley, J. Bohdansky, W. Eckstein, P. Mioduszewski, J. Roth, E. Taglauer, E.W. Thomas, H. Verbeek, K.L. Wilson, Nucl. Fusion **24**(S1), S9 (1984)
28. E.W. Thomas, Vienna: IAEA p. 94 (1984)
29. M.S. Chung, T.E. Everhart, J. Appl. Phys. **45**(2), 707 (1974)
30. *ITER Technical Basis, ITER EDA Documentation Series No 24, IAEA, Vienna 2002*

31. R. Marek, J. Straub, Int. J. Heat Mass Tran. **44**(1), 39 (2001)
32. A.T. Dinsdale, Calphad **15**(4), 317 (1991)
33. D.R. Lide, *CRC Handbook of Chemistry and Physics 80th Edition* (Taylor & Francis, 1999)
34. T.E. Stringer, Nucl. Fusion **12**(6), 689 (1972)
35. I.H. Hutchinson, Plasma Phys. Contr. F. **48**(2), 185 (2006)
36. S.A. Khrapak, A.V. Ivlev, S.K. Zhdanov, G.E. Morfill, Phys. Plasmas **12**(4), 042308 (2005)
37. C. Thornton, Z. Ning, Powder Technol. **99**(2), 154 (1998)
38. W. Goldsmith, *Impact: the theory and physical behaviour of colliding solids* (London: E. Arnold, 1960)
39. X. Li, P.F. Dunn, R.M. Brach, Aerosol Sci. Tech. **33**(4), 376 (2000)
40. R. Bridson, R. Fedkiw, J. Anderson, ACM T. Graphic. **21**(3), 594 (2002)
41. M.C. van Beek, C.C.M. Rindt, J.G. Wijers, A.A. van Steenhoven, Powder Technol. **165**(2), 53 (2006)
42. S.V. Klinkov, V.F. Kosarev, M. Rein, Aerosp. Sci. Technol. **9**(7), 582 (2005)
43. D. Shepard, in *Proceedings of the 1968 23rd ACM National Conference* (ACM, New York, NY, USA, 1968), pp. 517–524
44. G.F. Counsell, J.W. Connor, S.K. Erents, A.R. Field, S.J. Fielding, B. La Bombard, K.M. Morel, J. Nucl. Mater. **266–269**, 91 (1999)
45. P.N. Brown, A.C. Hindmarsh, L.R. Petzold, SIAM J. Sci. Comput. **15**, 1467 (1994)
46. L.R. Petzold, in *Scientific computing (Montreal, Quebec, 1982)* (IMACS, New Brunswick, NJ, 1983), pp. 65–68
47. S. Nordbeck, B. Rystedt, BIT **7**(1), 39 (1967)
48. S.W. Sloan, Adv. Eng. Softw. (1978) **7**(1), 45 (1985)
49. Cosine Distribution: `http://www.iue.tuwien.ac.at/phd/ertl/node100.html`
50. G.F. Matthews, J. Nucl. Mater. **438, Supplement**(0), S2 (2013)